Triggering Invisible Decays

Nicholas Sundstrom

February 2024

Daily Supervisors:
Dr. Kristof De Bruyn
Mick Mulder, PhD

First examiner: Dr. Kristof De Bruyn
Second examiner: Dr. Steve A. Jones

Masters Thesis

University Of Groningen
Netherlands

Contents

Abstract

The Groningen LHCb group is preparing to obtain the first measurement of the decay $B_c \to \tau\nu_\tau$ during the next data taking period of the Large Hadron Collider (LHC) at CERN. With a full detector output at a rate of 30Mhz [13], decisions to save or discard data must be made in real time while ensuring the recorded data is sufficient for performing offline analysis later on. The following thesis therefore will focus on the validation of software (called a trigger-line) written to identify the desired decay and trigger the LHCb detector to save relevant events for future analysis. Utilising the recently upgraded LHCb detector, the $B_c \to \tau\nu_\tau$ trigger-line has shown to efficiently reject background candidates when tested on simulated data sets. The results of this thesis provide sufficient evidence that the $B_c \to \tau\nu_\tau$ trigger is ready for implementation in the upcoming data collection period.

1 Introduction

Physics has always had the goal of building a theory to describe various dynamic systems. Classically physics has more or less succeeded, however through this journey, questions about the origins of the Universe and what happens at the limits of time and space have taken the forefront of physics research. This has led to two paths, either study the astronomically large or the infinitesimally small; with this thesis falling in the latter category.

Currently the most widely accepted theory about the origins of the Universe includes the Big Bang. An extremely powerful explosion from an infinitely dense and hot mass. Shortly after the Big Bang it is believed the first subatomic particles began to form in a violent plasma, and as we further understand the dynamics in such violent conditions the more conclusions can be drawn about the development and behaviours of these particles in our Universe.

This leads us to high energy particle physics, and more relevant to this thesis we will focus on collider physics. A subset of particle physics that focuses on colliding particles at extremely close to the speed of light in order to understand the dynamics of the subatomic particles that make up our Universe. These accelerators and collider experiments have been around since the mid 1940's. However it wasn't until the 1950's and 1960's that numerous new particles began to be observed. Slowly and systematically a new theory was created, this theory known as the Standard Model of particle physics gained widespread acceptance in the 1970's with the discovery of quarks. Since then the theory of the Standard Model has sat at the forefront of particle physics being able to describe the majority of particle interactions that we see today. However it does not account for everything that we have observed in our Universe. Notably the Standard Model fails to account for gravitational forces, and does not provide indications for the existence of dark matter and dark energy, phenomena whose effects have been observed. In spite of being the best known theory to date all physicists agree the Standard Model is not complete.

This is the current focus of most experimental particle physics, to rigorously test the predictions made by the Standard Model, and search for explanations of the so far, inexplicable. In the event that predictions do not match the experimental results then the theory needs to be modified. This is where the term beyond the Standard Model physics comes from, physics that will require additions to the current formulation of the Standard Model in order to explain.

At the forefront of testing the Standard Model is the Large Hadron Collider (LHC). The host organization CERN gets its name from a French acronym which translates to European Council for Nuclear Research. Founded in 1954 [5], with the goal to bring Europe to the forefront of fundamental physics research. Discussed in section 3.2 of this thesis, this accelerator hosts numerous experiments designed to further our understanding of nature at the smallest scales. Among these experiments, LHCb, a research collaboration working with the LHCb detector, focuses on further understanding the Standard Model through probing decays involving beauty quarks. With over 1600 individual participants across 98 institutes in 23 countries [12] the LHCb collaboration carries the original intent of CERN by uniting people with the common goal of subatomic research.

Among the 1600 individuals, numerous ideas of how to best probe the inner workings of the Standard Model through b quark decays are being explored every day. Over the years experimental measurements have both aligned and strayed from the Standard Model predictions laid out by theorists. Measurements exceeding a 5σ deviation from these predictions indicate the presence of new

physics, this for particle physicists is seen as the 'magic number'. However few measurements arise with an initial deviation of this magnitude, often physicists observe minor deviations and through further measurements these may converge towards our predictions or reach this 'magic number'. One of these measurements known as $R(D^{(*)})$ anomaly discussed in section 2.2 sits 3σ [9] from the Standard Model predictions. Taking a unique approach, the LHCb group at the University of Groningen aims to obtain further understanding of the an anomaly called $R(D^{(*)})$ by making the first ever measurement of a related decay $B_c \to \tau\nu_\tau$. The challenges involved in measuring this decay lie with its extremely short lifetime. This effectively means that prior to recent upgrades of the LHCb detector the decay was considered invisible, leaving it indistinguishable from any other decay in the detector. As part of this group, my contribution presented in this thesis, assists in authoring and validation of software that will aid in the first detection of the decay $B_c \to \tau\nu_\tau$, allowing LHCb to capture this event for further offline analysis.

2 Theory

In an effort to provide context to the experiment and analysis that will follow, below we will describe the leading theory of particle physics known as the Standard Model. The overarching goal of particle physics experiments being to validate or invalidate the Standard Model of particle physics. In addition section 2.2 presents an anomaly within the standard model the Groningen LHCb group aims to provide further insight to through the measurement of $B_c \to \tau\nu_\tau$.

2.1 Standard Model

The Standard Model of particle physics is the leading theory of particle physics, which provides a framework for the interactions of the elementary particles of our Universe. These particles, shown below, include fermions which make up the matter we interact with and define the forces through mediation of the bosons.

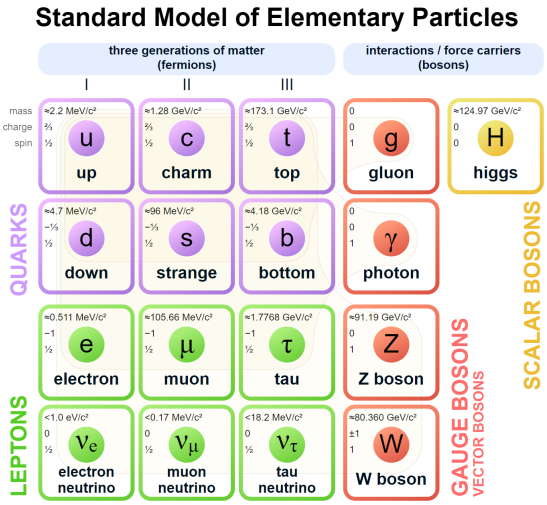

Figure 1: Standard Model of Particle Physics

Fermions are spin $\frac{1}{2}$ particles, which include of three generations of quarks (different quarks often referred to as different flavours) and leptons, with each generation heavier than the last. The quarks make up hadronic particles, pairs come as quark anti-quark pairs (denoted $q\bar{q}$) and are called mesons. These hadronic particles interact through the strong, weak, and electromagnetic forces, while the leptons do not interact with the strong force they do interact through the weak and electromagnetic forces (note neutrinos only interact weakly). This means that all of the fermions can interact with each other, and the way they interact with each other is mediated by the gauge bosons. The electromagnetic force is mediated by the photon, strong by the gluon, and the weak force by the W and Z bosons.

2.2 $R(D^{(*)})$ Anomaly

The Standard Model is composed of numerous symmetries that give physicists ideas as to how particles should interact with each other. One of the intrinsic symmetries is called lepton flavour universality (LFU). LFU indicates that coupling strengths of the leptons with the gauge bosons should only depend on the respective masses of each lepton generation, however experimental measurements have hinted that this may not be the case.

This has been shown through recent measurements of B meson decays which have deviated from their Standard Model predictions. Specifically the measurement $R(D^{(*)})$, is the branching ratio of $\bar{B} \to D^{(*)}\tau\bar{\nu}_\tau$ with respect to $\bar{B} \to D^{(*)}l\bar{\nu}_l$ where $l = \mu$ or e [4]. This is also written as,

$$R(D^{(*)}) = \frac{\mathcal{B}(\bar{B} \to D^{(*)}\tau\bar{\nu}_\tau)}{\mathcal{B}(\bar{B} \to D^{(*)}l\bar{\nu}_l)} \tag{1}$$

Combined 2D confidence level intervals of these measurements have shown deviations from the Standard Model predictions at the 3σ level as shown by averaging plots made by the Heavy Flavour Averaging group [9, 3] using data provided by numerous experiments.

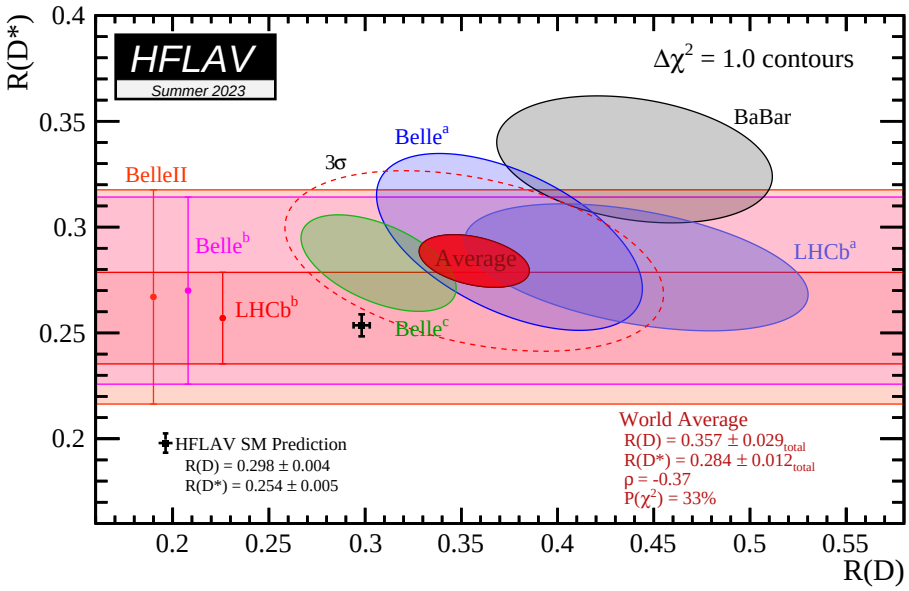

Figure 2: $R(D)$–$R(D^*)$ 2D Confidence Intervals [9, 3]

This hints at τ having a different coupling strength to that of the μ or e, opening the door for physics that violates LFU. This 3σ tension is a great hint for beyond the Standard Model physics and in order to understand this more, it must be probed. The Groningen LHCb group believes this can be done by first taking a closer look at the decay $\bar{B} \to D^{(*)}l\bar{\nu}_l$.

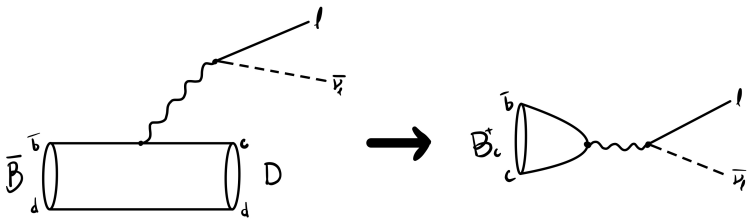

Figure 3: Isolation of Quark process in $R(D^{(*)})$

From figure 3 it is clear that these two different decays are described by the same underlying quark process. If one ignores the spectator quark and the hadronisation into mesons the two diagrams are simply 90 deg rotations of each other. Thus from $\bar{B} \to D^{(*)} l \bar{\nu}_l$, the decay $B_c \to l \bar{\nu}_l$ appears. The Groningen LHCb group believes that the next step to understanding LFU can be done through comparing experimental measurements of the branching fraction, $\mathcal{B}(B_c \to \tau \bar{\nu}_\tau)_{EXP}$, to its Standard Model predictions, $\mathcal{B}(B_c \to \tau \bar{\nu}_\tau)_{SM}$. The logical next step is to determine how these measurements will be performed.

3 LHCb Experiment

The following sections will give an overview of the experimental setup that the LHCb Detector is a part of. To do this we will give an introduction to CERN and the series of accelerators hosted on site.

3.1 LHC

The Large Hadron Collider, commonly referred to as the LHC, is the largest particle accelerator and collider at CERN and currently in the world. This massive 27 kilometer long ring is housed 100 meters underground in tunnels that sit under the Franco-Swiss border.

As stated in the name, the LHC provides proton-proton (pp) collisions, which produce numerous exotic particles to be measured increasing the understanding of the Standard Model. Through accelerating bunches of protons $\sim 3m/s$ slower than the speed of light and smashing them together, scientists are able to study exotic particles in the most controlled environment ever built.

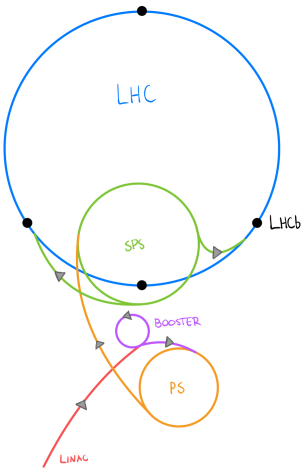

Figure 4: proton injection steps

As the LHC cannot bring proton bunches up to 7 teraelectronvolts (TeV) on its own, steps are required in the process to accelerate and optimize the proton bunches so that the collisions are as efficient as possible. The process of accelerating protons requires a rapidly switching electromagnetic field called an RF (radio frequency) field, to boost the protons through the accelerator. In addition to this focusing magnets further tighten the proton bunches to increase their interaction cross-section prior to collision. Protons begin their journey shown in figure 4 through the Linear Accelerator (LINAC) next sent through the Proton Synchrotron Booster (PBS) bringing the protons to 2 GeV, where they are brought into the Proton Synchrotron (PS) where the beam is brought up to 26 GeV [14]. From here they are sent to the Super Proton Synchrotron (SPS) accelerating the proton beam up to 450 GeV [15] and splitting the beam into two separate beam pipes as they are sent into the LHC. The LHC does the final push squeezing the proton bunches into a tighter group and accelerating them to just below 7 TeV. This means that the center of mass

energy reaches a total of just below 14 TeV. From collisions at this energy protons explode into a shower of subatomic particles some of which traverse the detectors placed at the interaction points of the collider to be measured. On the LHC ring to the right of the SPS, the LHCb Detector, one of the four main detectors on the LHC is labeled in figure 4. This will be the subject of the following section.

3.2 LHCb Detector

As stated above the LHC hosts four main detectors on the LHC which are all faced with the same problem of extracting the relevant data from a flurry of particles produced in pp collisions occurring 30 million times per second. The LHCb experiment and collaboration focuses on the search for new physics through studying decays involving b quarks, which gives the name *LHCb*. The detector features a unique design in order to accomplish this. The other three major detectors at LHC opt for a 4π design meaning their detectors host a cylindrical shape with collisions occuring near the center, providing nearly complete directional coverage. This on the surface, sounds like the optimal choice for any detector. However, the LHCb detector layout shown in figure 5, is known as a forward arm spectrometer.

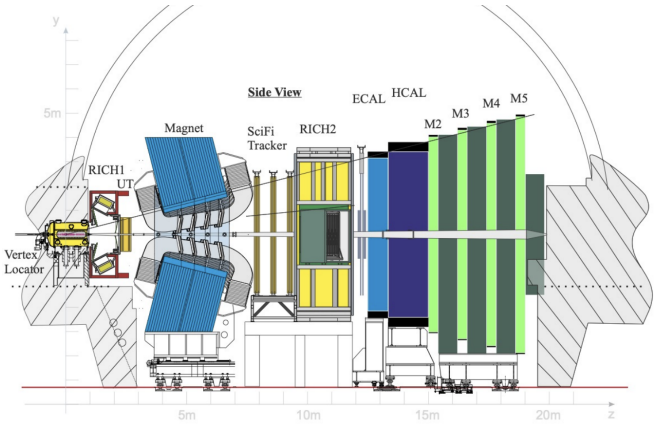

Figure 5: Schematic overview of the LHCb subdetectors [2]

This geometrical configuration was chosen as b-hadrons are largely produced in a forward and backward cone about the interaction point [6]. With collisions occurring at the Vertex Locator (VELO), the detector provides detailed tracking information and particle identification within the pseudo-rapidity range $2 < \eta < 5$ [6]. Particle identification takes multiple measurements into account throughout the detector. Observing the curve of particles passing through the magnet provides charge and momentum information, in addition the lack of a track indicates a neutral particle. Particles predominately interacting electromagnetically are deposited in the electromagnetic calorimeter, providing mass measurements, while others will be deposited and measured in the hadronic calorimeter. The path a particle takes as well as its lifetime can be observed through particle trackers, if its decay vertex can be reconstructed from its decay products. For example a muon can be identified as a track passing through the entirety of the detector even before being measured by the muon chamber at the far end of the detector.

Integral to the tracking system is the detector's Vertex Locator. Through providing precise coordinate measurements near the interaction point, the VELO can detected displaced secondary vertices which are a key sign of a b-hadron decay. In the most recent upgrade of the LHCb detector the geometry of the VELO was adapted to allow for a closer approach to the interaction point.

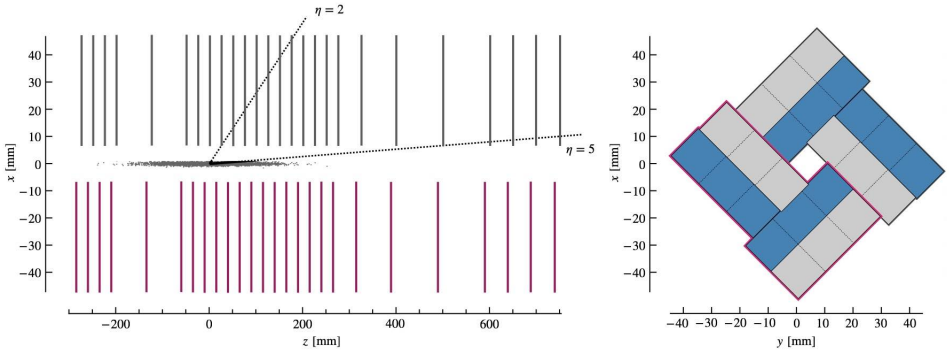

Figure 6: LHCb Vertex Locator. Left: Cross section of modules. Right: VELO modules enclosing beam line (left module outlined in purple, right module with no outline). [2]

The new geometry, shown on the right in figure 6, features two 'L' shaped components (left hand component outlined in purple) that join to create a square around the beam line. The beam line is perpendicular to the XY plane. This configuration has reduced the previous point of closest approach from $8.2mm$ to $5.1mm$ [2]. This has opened up the possibility of directly searching for a B meson hit in the VELO. As will be shown in the $B_c \to \tau\nu_\tau$ reconstruction section, this increases the accuracy of correctly identifying and sorting desired events in the detector.

3.3 LHCb Data Flow

In order to make accurate measurements in particle physics, not only does it help to have high resolution detectors, but increasing the amount of data reduces the experimental uncertainty. This is especially relevant when talking about exotic decays like $B_c \to \tau\nu_\tau$. With recent upgrades increasing the luminosity (event rate) of the LHC, more data than ever before is available to be analysed. However this presents a new problem, namely how does one handle all of this data?

To put into perspective the magnitude of data the LHCb group is dealing with: The bunches of protons circle the LHC at a rate of 40MHz, providing the LHCb data at a rate of 30MHz [13]. The full detector readout of particle interactions within the detectors lead to an output of 5TB/s [13]. This is a massive amount of data, and without any type of filtering it would be impossible to save the data for any further offline analysis.

To handle this volume of data we introduce the idea of a trigger. One can think of a trigger as a checklist that iterates over each event in the detector, and if enough boxes in that checklist are filled, the event is considered interesting and the data corresponding to that event is saved. Taking into account that hundreds of analysis groups are running at the same time, there are numerous triggers each called a trigger-line.

The full trigger consists of two steps, the first called HLT1 (High Level Trigger 1) with the main goal of reducing the data flow so that further event specific and more computationally complex selection processes can occur during the second step, HLT2 (High Level Trigger 2).

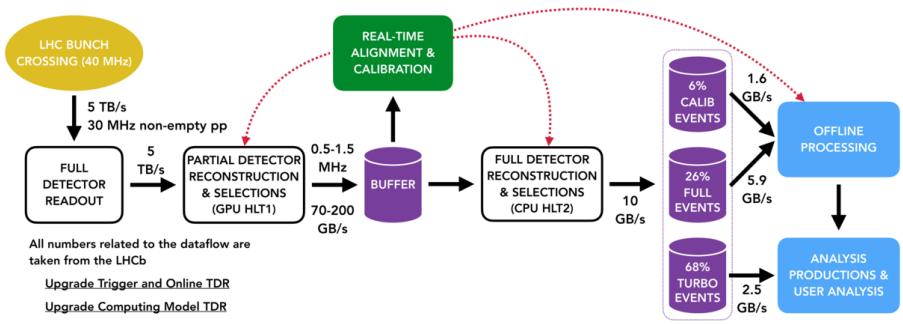

Figure 7: LHCb Data Flow [13]

The general requirements for the HLT1 are such that events that align with the broad goals of an LHCb analysis are passed through the data pipeline for further analysis. This selects events primarily based on two physical signatures present in decays listed below [2].

- Tracks displaced from the primary vertex.
- Leptons, primarily muon tracks, with or without a displaced vertex.

From these two criteria in HLT1 the amount of data sent through the pipeline is reduced by a factor of ~ 25. From here the partially reconstructed event along with calibration data, is passed to the HLT2 where full event reconstruction takes place. We consider an event to be reconstructed within the context of the HLT2, as having 70% of the hits associated with a track are correctly accounted for [7]. For simplicity in a track of 10 hits 7 are properly identified and matched to the track. In addition to this, with a slight delay between HLT1 and HLT2, the calibration data from HLT1, allows for re-alignment of detectors; enabling analyses to begin hours following data taking as opposed to months due to the amount of data that would need to be calibrated. From this point each event passes through $\mathcal{O}(1000)$ [10] selection trigger-lines which make the final decision on whether the event in question should be written to disk storage, and to which analysis group the data should be allocated to. The specifics of which will be defined in the next section.

4 LHCb Software Stack

The LHCb software stack is a package which encompasses all steps of the process from detector read-out to the creation of histograms for presentation. Relevant to the topic of this thesis it provides the software to test trigger-lines in a simulated environment without requiring the full detector and reconstruction computer farm at CERN. Used in this thesis, for triggering specific decay modes, is the software package Moore [10]. Moore has the role of executing the trigger-lines with provided parameters on simulated or real data, and providing statistics as to how well the given trigger-line performed.

4.1 Triggering Data

A simple way to think of a trigger-line, as stated above, is to imagine it as a checklist. Once those requirements on the checklist are met the corresponding event is passed down the data pipeline. Any events that do not, are removed, or cut from the data set. For HLT1, this is a generic checklist that has the primary purpose of reducing the data flow so that more computationally intensive triggers can further sort the data. The focus of this thesis however lies within HLT2, these trigger-lines are decay specific. This means more requirements to differentiate each event from one another. These event specific parameters can be divided into two general groups, the first regarding the topology of the decay and the second involves determining the particles within the decay.

Starting with the more tangible of the two, the topology of an event looks at reconstructing the decay starting at the final products and working towards the primary vertex. Where the decay in time occurs as, $pp \to B_c \to \tau \to 3\pi$ one can view the reconstruction process occurring in reverse as, $3\pi \to \tau \to B_c \to pp$. Discussed in the LHCb detector section, the layout of the detector has layers allowing particles to be differentiated along their flight through the detector. Figure 8 depicts a simplified view of the VELO and what the reconstruction algorithm provides.

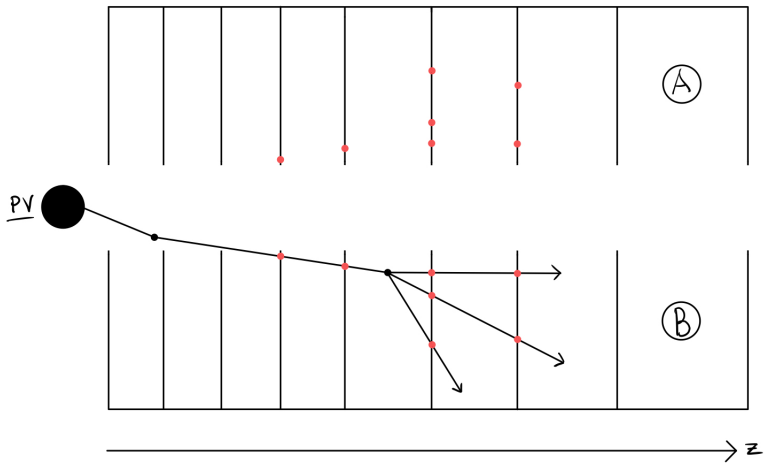

Figure 8: Region A: No software intervention. Region B: With reconstruction software.

As shown in figure 8 without any software intervention, the detector only provides disconnected particle hits as they interact with the sub-detector modules. However the above example is extremely simplified, in actuality this reconstruction needs to disentangle millions of tracks accurately. Furthermore with a data rate of 30MHz, a robust trigger-line is required to not stall data taking process.

In conjunction with the tracking systems, particles undergo numerical measurements. This for example could involve, measuring deflection angles through magnets, or energy deposited in a calorimeter. This allows for us to add constraints on what particles to accept i.e. disregarding particles below a certain energy. Through employing combinations of measurements by the sub-detectors we are able to identify particles to further aid the reconstruction process. In addition through adding up the four-momentum vectors of daughter particles of the same vertex, we are able, with the help of additional tools outside the scope of this thesis, determine the parent particle and save, or discard, the corresponding decay.

5 Triggering $B_c \to \tau\nu_\tau$

Throughout this section we discuss the process of selecting the decay $B_c \to \tau\nu_\tau$. First through introducing the shape of the decay, we are able to understand the motivation for the methods of detection.

5.1 Topology of Decay

As mentioned in the introduction the title of this thesis *Triggering Invisible Decays*, alludes to the nearly invisible nature of the $B_c \to \tau\nu_\tau$ decay from the viewpoint of the LHCb detector.

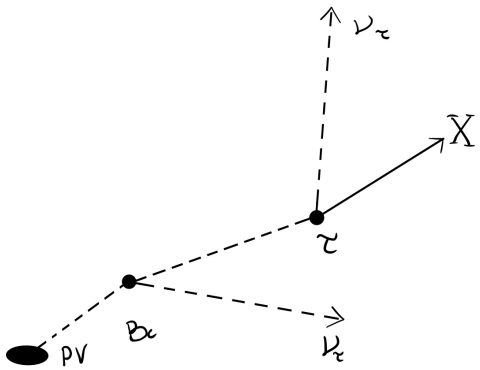

Figure 9: $B_c \to \tau\nu_\tau$ decay overview. Solid lines represent what is detectable using standard methods. Dotted lines represent what would be invisible implementing standard methods.

In Figure 9 above the decay topology is shown, where a dashed line refers to a particle that would not be observed by the detector using methods present in standard trigger-lines. It is important to note that two of the tracks represented are neutrinos, which rarely interact with matter, therefore must undergo indirect detection through Cherenkov radiation at specially designed detectors like those found at KM3Net [11], these capabilities are beyond those of LHCb. This leaves three tracks that have the ability to be observed by the detector, the path from the primary vertex to the B_c, the path from the B_c to the τ, and finally the τ to its decay products. Here the τ decay product, indicated with an 'X', represents an arbitrary particle. Through selecting a proper decay mode, ensuring the particle 'X' is stable enough, this is likely the only portion of the decay that can be identified using standard methods present in trigger-lines. This is due to the lifetime of the B_c meson and τ being on the order of $(0.510) \cdot 10^{-12}$ seconds [17] and $(2.903) \cdot 10^{-13}$ seconds [17] respectively, both of which are not long enough to reach a substantial point in the detector to be measured. However, particle 'X' can still undergo mass measurements, as stated earlier, through energy deposited in a calorimeter or by measuring its deflection angle through a magnetic field. This then provides more information allowing the track for particle 'X' to be tagged as a specific particle beginning our reconstructed process. Furthermore using the four-momentum vectors of decay product(s) ('X') we can likely determine the parent particle in the process. As a simplistic example if the reconstructed mass is close to the mass of the τ at 1.777MeV, ignoring corrections to account for the neutrino, then the parent particle would be assumed to be a τ.

Before reconstructing the decay above a decision needs to be made about what particle 'X' is. This is because trigger-lines are decay mode specific, therefore we cannot write one line that finds every τ that comes from a B_c. Therefore a selection needs to be made that fills the criteria of having a large signal to background ratio, decaying into long-lived particles, and preferably charged particles. The first criteria is rather self explanatory, when a decay is more abundant with respect to its background, it is easier to obtain more data for research, disregarding other factors. Second, long-lived particles have a greater chance of passing through multiple stages of the LHCb tracking system, providing higher resolution tracks allowing for more accurate reconstruction. Finally, limiting our search to a τ decay with charged particles means that they will produce a track in the VELO allowing for further increased reconstruction resolution.

With the above criteria in mind, the decay $B_c \to \tau\nu_\tau \to \pi^+\pi^-\pi^+\bar{\nu}_\tau$ was selected. Given the large branching ratio of $(9.31 \pm 0.05)\%$ [17], the long lifetime of the charged pion at $(2.6033 \pm 0.0005) \cdot 10^{-8}$ seconds, enough to traverse the whole detector, and the number of pions in the decay, all criteria are met. The view of our specified decay is shown below.

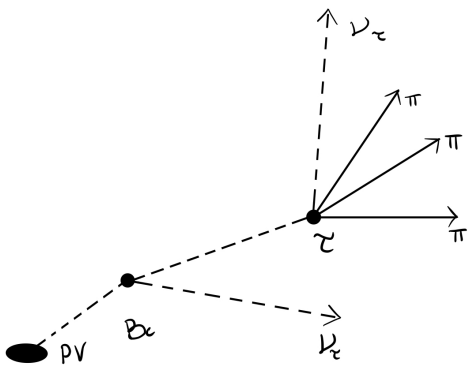

Figure 10: $B_c \to \tau\nu_\tau \to 3\pi\nu_\tau$ decay topology

As shown in figure 10, using methods implemented in a standard reconstruction algorithm, the 3 pion tracks allow us to determine the vertex of the τ. The process of doing this, will be explained in the following section.

5.2 General cuts

For this thesis, 'General Cuts' are defined as cuts that can be implemented in the previously used trigger-lines at LHCb. This primarily focuses on the τ reconstruction by means of the 3π. It is important to note that these cuts are performed in succession, by implementing computationally taxing cuts later in the process we reduce the number of candidates that need to undergo time consuming calculations. Prior to any mass cuts, a particle identification step is performed. This process entails a likelihood value being applied to particles passing through each sub-detector representing a probability of a particle being a kaon, pion, electron, or muon.

This particle identification (PID) value acts as the first cut, in our case allowing the isolation of just pion candidates. From here, the first selections occur on the identified pion candidates

called the two body selection. This function is called to comb through each pion candidate and record each set of two pions who's combined mass is less than that of a $m_\tau - m_\pi$. The only other constraint here is that the pion combinations can only include at most one negative pion. The exact values used in the code to perform cuts is provided in three tables one below each step of the reconstruction process.

Two-Body Reconstruction	
Mass Cut	1670 MeV

Following collection of possible pion pairs we move to adding a third pion candidate to each of the pairs to conduct the three body selection process. In addition to the following parameters, the pion combinations have to be $\pi^+\pi^-\pi^+$, in order to conserve charge. The three body selection also employs more requirements in addition to the mass cuts similar to the two body selection. The first parameter applied to the three body reconstruction ensures a displaced vertex by removing candidates with low transverse momentum (momentum perpendicular to the beam line axis). We then employ a second mass cut slightly above the mass of the τ particle to account for resolution on measurements, this also helps reject backgrounds from D-mesons (combination of c with u,d,s quark). Following this we include a distance of closest approach (DOCA) cut, in which pion tracks are compared to each other ensuring that the candidates likely stemmed from the same vertex [16].

Three-Body Reconstruction	
P_T	> 4500 MeV
Mass Cut	1825 ± 50 MeV
DOCA	< 0.2 mm

The final selection process called the vertex based selection helps to further reduce the background. This selection begins with a higher transverse momentum cut and and tighter mass cut. This is followed by a χ^2 cut on the vertex of the three pions. Following this a cut on the flight distance of the particle is made ensuring it is large enough. The final cut is another χ^2 cut however this time it is the χ^2 of the impact parameter, defined as the distance between the primary vertex and the relevant track at their closest point [1].

Vertex Fit	
P_T	5 GeV
Mass Cut	< 1825 MeV
χ^2_V	< 16
Flight Distance	> 4.0 mm
χ^2_{IP}	> 9

5.3 B-Hit Detection

From the section above, we reconstructed the τ decay vertex, through the pion hits found in the detectors tracking systems. Referring back to figure 10 this leaves two tracks (excluding the neutrino tracks) unaccounted for. In an effort to reduce background presented from other pion final states a more complete picture of the decay must be obtained. For this reason we will introduce a

B-Hit Detection algorithm, with the goal of identifying and including a charged B meson or τ hit in the VELO to the now known τ decay vertex. This builds a more complete picture of the decay, allowing us to fill in the gap between the PV (primary vertex) and τ vertex. It is important to note that within the VELO it is not possible for us to distinguish between a hit from the B meson or a τ and both are desired information for the trigger-line, however for the purposes of simplicity the term B-Hit will encompass both possibilities.

The process of identifying a B-Hit is done by creating a cylindrical search window (radius .5mm) starting and centered at the τ decay vertex and extending towards the primary vertex. This identifies VELO modules intersected by the cylinder centered along the line connecting the primary vertex and secondary vertex (PV-SV line) refered to as a crossed module. One may notice that the τ vertex could be considered the tertiary vertex, the first being the PV, and the second belonging to the B meson. However, in practice as we are not able to distinguish between the B meson and τ, we ignore the B vertex, and refer to the τ as the secondary. Following the identification of crossed modules, the closest module to the τ decay vertex in z with a hit (or hits) falling within the search window is parsed. Of the identified hits, the hit closest to the center of the search window (at this point also the PV-SV line) is selected, and once selected, the search cylinder shifts with the center of the cylinder connecting the τ vertex to this newly identified hit. Through shifting the search window we are able to use the same algorithm and parameters for identifying hits, being those closest to the center of the cylinder. Otherwise two algorithms would be required, first being a hit closest to the PV-SV line, and second hits closest to the identified τ track. By reusing our algorithm for two different cylinder positions we reduce the chance of introducing errors in code as well as expediting the debugging process when errors do arise. It is important to note that during live data taking only, one hit per module (the closest to the center of the search window) is passed by the trigger-line and all other hits on the VELO are accessible later during offline analysis.

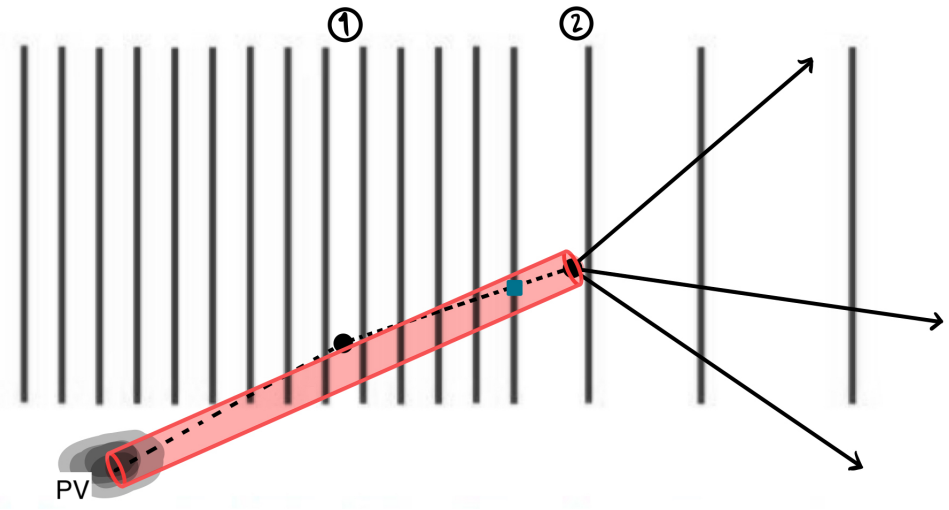

Figure 11: Search window before identifying heavy flavour hit

This is shown in figure 11, the position marked PV is our primary vertex where proton collisions occur, point one marks the decay vertex for the B_c and point two marks the τ decay vertex. In

figure 11 a hit has not been identified yet, therefore the cylinder points towards the primary vertex. The following figure shows the shift in the search window once a hit is identified.

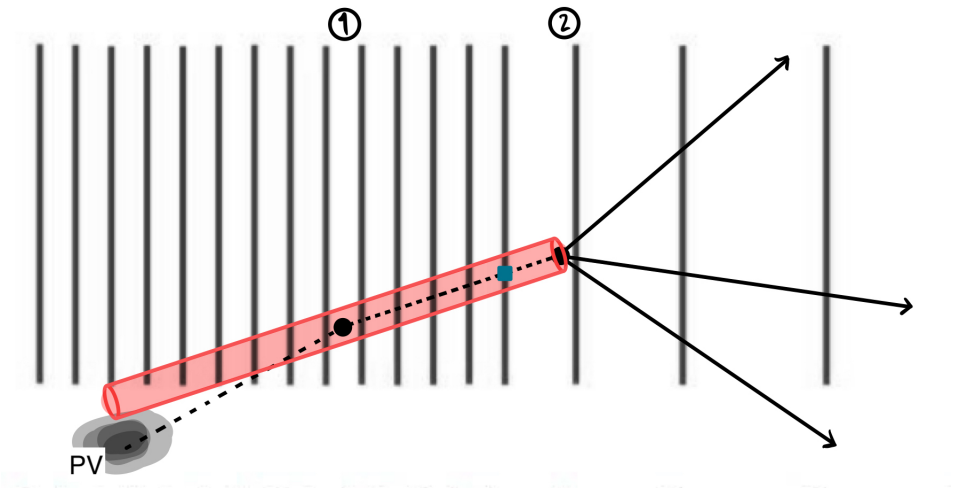

Figure 12: Search window after heavy flavour hit identification

Shown above in figure 12, the search window has now shifted and points along the path of the newly identified hit as compared to figure 11 where the cylinder points towards the PV. As stated previously the following modules are iterated through and the B_c and τ tracks are built. In the event a hit is not identified in the first module prior to the τ decay vertex the line of sight to the primary vertex is still used until a hit is identified. In contrast with the previous section (5.2) finding a B-Hit is not a cut on the trigger-line. In the event that 0 hits are found along the PV-SV line but every other criteria passed, the event is not thrown out. However through finding a B-Hit in the VELO we gain more information on the angle of the B meson to τ vertex, allowing us to improve our corrected mass measurements. For this reason the B-Hit algorithm is still calculated with the rest of the trigger-line. This way the B-Hit algorithm only serves to benefit the analysis.

6 Validation of $B_c \to \tau\nu_\tau$ Trigger

6.1 Validation Process

Prior to implementing the trigger-line for live data taking, it is important to guarantee each portion of the code is working as intended. This is typically conducted over Monte Carlo simulated data that is processed and reconstructed as real data before being used for trigger-line validation. Uniquely this simulated data includes the 'truth' values, allowing testers to confirm that the proper particle was reconstructed. This can be thought of as an answer sheet that would be given, to a grader for an exam. During the analysis in this thesis our 'exam grader' is a function included in our reconstruction called 'MC-Checker'. This provides statistics comparing the truth information with the trigger output. If we incorrectly pair a VELO hit to a reconstructed τ vertex, we are able to see and modify our line. Due to the τ vertex reconstruction being well understood by LHCb, the 'MC-Checker' algorithm was not included for this portion of the cuts. The outputs provided are defined and discussed in the following section.

Once the trigger-line is working as intended it is important that the line operates within its computational budget, while removing enough background without compromising desired data. The concept of computational budget largely encompasses two main criteria, ensuring the computational time and data-stream are within an allocated budget. The first criteria is typically handled by making sure that the computationally complex processes are handled later in the trigger-line to avoid running over all incoming data. As in section 5.2 the most complex cuts imposed on the data, (χ^2 and flight distance cuts) were run last, ensuring the majority of irrelevant data had already been disregarded by then. The second criteria involves the trigger not passing too much data through to be stored for offline analysis, as the storage and data-stream capabilities of LHCb are finite. This criteria varies providing different analysis across LHCb with varying budgets, however a more efficient trigger should without problem not weigh heavily on the data-stream.

6.2 *Bc2TauNu* Trigger-line Output

The output shown below will be presented in the following order, the output from the general cuts, the B-Hit algorithm, and finally the rate of the trigger-line. For context due to a lack of resources on the LHCb, computing side the data set used for the following output only contains 299 events. This in the future would be increased given the work done by the Groningen LHCb group.

Starting with the outputs of the general cuts, as discussed in section 5.2, these cuts consist of a two-body and three-body reconstruction, followed by a cut on the vertex. What we are looking for in the output, is a large reduction in data, prior to the 'Vertex-Cut'. With this cut being the most computationally complex it is important to reduce data prior to not create a bottleneck the data flow.

Table 1: 3π Reconstruction Cuts

Reconstruction Step	Candidates	Passed	mean/eff* ± rms/err*
Two-Body	8662	5160	59.570% ± 0.5273%
Three-Body	10792	128	1.186% ± 0.104%
Vertex-Cut	128	87	67.968% ± 4.124%
# passed	299	78	26.086% ± 2.539%

In the above table starting with row one, we can see that there are 8662 possible two-body reconstruction combinations, and of those 5160 passed the parameters outlined in 5.2. The three-body reconstruction has 10792 possible combinations with only 128 passing this more restrictive cut. It is important to note that in the three-body reconstruction the two-body pairs from the previous step may have multiple third particle possibilities, this is why the number of candidates increases after the two-body reconstruction. Finally the vertex-cut is given the 128 candidates from the three-body reconstruction section and of those 87 pass the cut on the vertex. The final row of the table indicates the number of events rather than individual candidates that pass and are saved for further analysis, the difference is due to multiple candidates occasionally coming from the same event. From this table we can clearly see that the majority of data has been excluded prior to the computationally complex 'Vertex-Cut'. As the reconstruction methods and values used for this section of the trigger-line have been used in previous LHCb analysis, it can be assumed that τ vertex selections are made as intended.

The following table presents the output of the B-Hit algorithm, this is run over the same MC truth data used in the previous table. Following the table explanations of each row will be given.

Table 2: B-Hit algorithm output

Counter	#	sum	mean/eff* ± rms/err*
Final state (FS): reco'd	299	117	39.130% ± 2.822%
Final state (FS): sel'd | reco'd	117	53	45.299% ± 4.602%
Has HF track | sel'd FS & HF reco'ible	34	33	97.059% ± 2.898%
True hit on track | sel'd FS & HF track	47	44	93.617% ± 3.566%
HF track: MC-matched | sel'd FS & HF reco'ible	34	29	85.294% ± 6.074%

The first row of table 2 shows the number of $B_c \to \tau\nu_\tau \to 3\pi\nu_\tau$ final states that were reconstructed, here 117 of 299. The final state relates to how many 3 π vertices were reconstructed. The following row (2) takes those reconstructed final states and checks how many were properly selected (tagged) as $\tau\nu_\tau \to 3\pi\nu_\tau$ candidates using the parameters from the selection cuts from section 5.2. The next row (3) looks at the the number of tagged final states that have a heavy flavour track (B-Hit) that can be reconstructed and connected to the pion vertex. It is important to note that this does not mean that the B-Hit was correctly paired with the reconstructed pion vertex, but that of 34 reconstructed pion vertices 33 have a potentially reconstructible B or τ track on the VELO modules. This also tells us that 29 of these events where a final state was selected, did not have a hit from a B or τ on a VELO module. The following row (4) compares the number of total B-hits, 47, to those that were identified and associated with a selected final state with a heavy flavour track, 44, by the algorithm. With 47 B-Hits in 34 total events we see see that some events contain multiple hits on VELO modules, furthermore we can assume the reason not all 47 were identified was due to the fact that some (in this case 3) fell outside of the search window.

The final row (5) indicates the number of selected final states with a reconstructible heavy flavour track that are correctly matched to a MC event. This uses the true value that comes from the MC simulated data and compares it to what the trigger-line was able to interpret. In this case 29 of 34 were reconstructed identically to the event in the MC data. If we compare this with row 3, we can see that 29 of the 33 events with reconstructible heavy flavour tracks were properly matched to a τ vertex. This means that 4 were not properly matched, meaning a τ vertex was paired with another charged particle passing through the VELO.

Each of these values are important and tell a story of how well the algorithm is able to find hits associated to the pion vertex. However the fourth parameter in the above table *'True Hit on Track | sel'd FS & HF track'* corresponding to the number of heavy flavour hits the search window is able to identify, we can use this parameter to observe the effects of a different search window sizes. If one recalls the default search window was set at 0.5mm, which has proven to work well with the data shown above, as it is able identify 93.6% of the heavy flavour hits from a selected pion vertex. However it is important to understand how both a larger and smaller search window perform. This will give insight as to what the best search window size may be, increasing the size in theory would increase the chance of finding a heavy flavour hit, but with this comes more data that must be parsed. Below is a plot showing the efficiency of identifying heavy flavour (HF) hits the search window at different radii. This is defined as the identified heavy flavour hits in a search window, divided by the total heavy flavour hits on VELO modules.

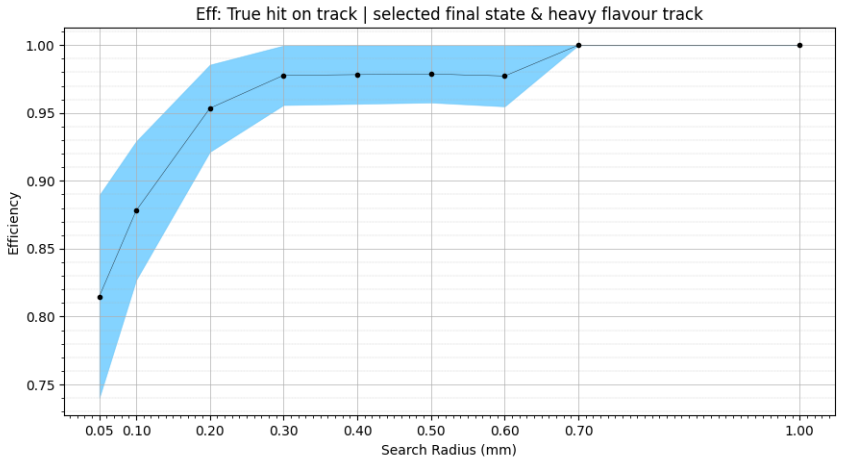

Figure 13: True hit identification efficiency

From figure 13 we can see that reducing the search window size to .3mm does not reduce the efficiency of identifying HF hits along the track compared to at .5mm and it does so without increasing the error. In addition to this, increasing the size of the search window does increase the efficiency, eventually identifying all HF hits associated to reconstructed final states. However the situation becomes complicated when we look at the individual counts that make up the above efficiency.

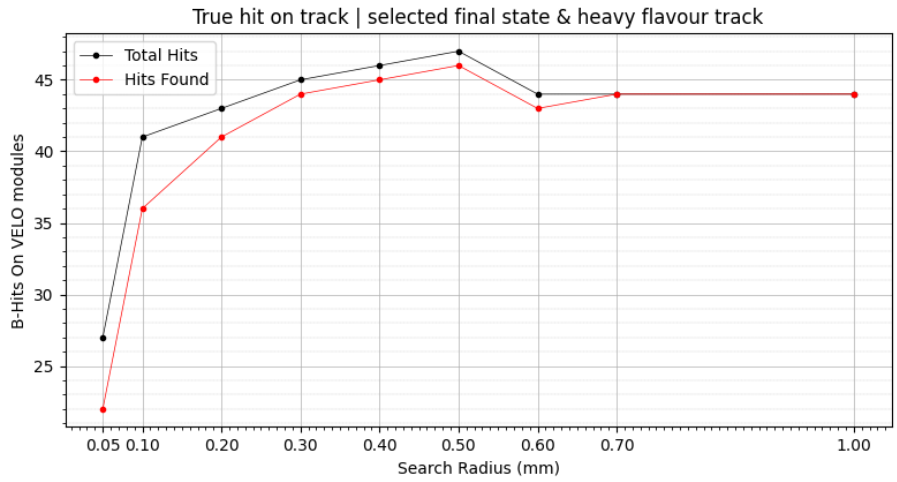

Figure 14: Total counts of heavy flavour hits on VELO modules

From figure 14 we see that on the low end for search window radius the algorithm acts as one would expect. With a radius of .05mm we find significantly less counts than we would at a search radius 10 times that value. However increasing the search window radius decreases not only the total counts for heavy flavour hits on VELO modules but the number of hits found. This works against ones intuition where we would expect more hits as the search window increases, until it eventually plateaus when it encompasses every heavy flavour hit on the modules. At the time of writing this thesis these abnormalities are being investigated and should become clearer if provided a larger data sample. However the decision has been made to stay at .5mm search window where the algorithm to be working as intended, as well as not require a B-Hit for an event to be saved, using this algorithm more as a tool for further analysis. In the event that the bandwidth limit is passed, it is possible to reduce the size of the search window to .3mm, likely eliminating background in larger data sets. The values shown when run over Monte-Carlo data, indicate that the trigger-line is largely working as desired, correctly identifying the desired event and discarding others.

As discussed in the previous section it is also important that the trigger-line operates within a data budget, for the *Bc2TauNu* trigger-line, this sits at 1kHz. In order for us to validate that the trigger-line operates within the bandwidth parameters, the trigger-line needs to be run over minimum bias data. The name minimum bias, refers to the fact that applying a cut on data introduces some bias to the data that passes that cut. For example a high P_T cut results in data biased with only high transverse momentum. From this we can deduce that minimum bias data is data that passes the least restrictive cut, resulting in a large portion of the inelastic cross section of proton-proton collisions [8]. When executing over minimum bias data regarding the *Bc2TauNu* trigger-line, we look at how much data the general cuts allow to be saved, as we are not cutting on any heavy flavour hit requirement.

After running the trigger-line over $14,983$ minimum bias events, 9 events passed and would be saved for offline analysis. Using the rate given in the data sample (*'upgrade_minbias_hlt1_filtered'*) of 1.65 MHz, we can calculate what the output rate would be.

$$\frac{9}{14983} \cdot 1.65MHz = .991kHz \tag{2}$$

This sits closely below our 1kHz requirement. However if this needs to be reduced further, the group has the option to tighten constraints on the τ reconstruction, or include the requirement of the B-Hit.

7 Conclusions and Outlook

From the previous section it can be concluded, in the event of a heavy flavour hit on a VELO module and a reconstructed τ vertex, a full reconstruction of the $B_c \to \tau\nu_\tau$ decay is possible. In addition the *Bc2TauNu* trigger-line fulfills the bandwidth requirements to be incorporated in the next data taking period of the LHCb experiment. With these conditions met it is clear that the LHCb Groningen group should expect the first direct measurements of the $B_c \to \tau\nu_\tau$ with the implementation of this trigger-line.

In addition to a positive outlook for the Groningen LHCb group, the contents of this thesis can open the door for further implementation of similar algorithms. With the upgraded LHCb detector being so new, it is likely LHCb physicists will have many analyses previously deemed impossible to look forward to.

8 Acknowledgements

I would like to thank those at KVI Groningen for providing a friendly environment with loads of coffee breaks.

Andrej and Briain, for inspiring me.

Mick Mulder, Kristof De Bruyn, and Maarten Van Veghel for their wealth of knowledge and guidance throughout my project.

MD, Jan, and Nikos for providing lots of laughs.

Marcel Merk and LHCb Nikhef for the guidance.

And thank you to my family and Eva for believing in me and bringing me to Groningen.

9 References

[1] R. Aaij et al. "Performance of the LHCb Vertex Locator". In: *JINST* 9 (2014), P09007. DOI: 10.1088/1748-0221/9/09/P09007. arXiv: 1405.7808 [physics.ins-det].

[2] Roel Aaij et al. "The LHCb upgrade I". In: (May 2023). arXiv: 2305.10515 [hep-ex].

[3] Yasmine Sara Amhis et al. "Averages of b-hadron, c-hadron, and τ-lepton properties as of 2021". In: *Phys. Rev. D* 107.5 (2023), p. 052008. DOI: 10.1103/PhysRevD.107.052008. arXiv: 2206.07501 [hep-ex].

[4] Debjyoti Bardhan, Pritibhajan Byakti, and Diptimoy Ghosh. "A closer look at the R_D and $R_{\{}D^*\}$ anomalies". In: (Oct. 2016). DOI: 10.1007/JHEP01(2017)125. URL: http://arxiv.org/abs/1610.03038%20http://dx.doi.org/10.1007/JHEP01(2017)125.

[5] CERN. *Where did it all begin?* 2024. URL: https://home.cern/about/who-we-are/our-history.

[6] LHCb collaboration. "Technical Design Report". In: (2018).

[7] Rutger Mark van der Eijk. "Track reconstruction in the LHCb experiment". In: (2002).

[8] Rick Field. "Min-Bias and the Underlying Event at the LHC". In: (Oct. 2011). URL: http://arxiv.org/abs/1110.5530.

[9] HFLAV. *HFLAV summer 2023 preliminary data rdrds.* 2023. URL: https://hflav-eos.web.cern.ch/hflav-eos/semi/summer23/html/RDsDsstar/RDRDs.html.

[10] LHCbDoc. *Moore Framework Documentation.* 2024. URL: https://lhcbdoc.web.cern.ch/lhcbdoc/moore/master/index.html.

[11] Annarita Margiotta. "The KM3NeT deep-sea neutrino telescope". In: (Aug. 2014). DOI: 10.1016/j.nima.2014.05.090. URL: http://arxiv.org/abs/1408.1392%20http://dx.doi.org/10.1016/j.nima.2014.05.090.

[12] LHCb Secretariat and Grey Book Secretariat. *CERN Grey Book database.* 2024. URL: https://greybook.cern.ch/experiment/detail?id=LHCB.

[13] LHCb Starterkit. *LHCb data flow in Run 3.* 2022. URL: https://lhcb.github.io/starterkit-lessons/first-analysis-steps/dataflow-run3.html.

[14] *The Proton Synchrotron — CERN.* URL: https://home.cern/science/accelerators/proton-synchrotron.

[15] *The Super Proton Synchrotron — CERN.* URL: https://home.cern/science/accelerators/super-proton-synchrotron.

[16] Maarten Van Veghel. "Pursuing forbidden beauty: Search for the lepton-flavour violating decays B0 $\rightarrow$ e$\pm$ $\mu\mp$ and Bs0 $\rightarrow$ e$\pm$ $\mu\mp$ and study of electron-reconstruction performance at LHCb". In: (July 2020). DOI: 10.33612/diss.128123609. URL: http://hdl.handle.net/11370/98900ef0-a602-414f-9936-1c2011e6696a.

[17] R. L. Workman et al. "Review of Particle Physics". In: *PTEP* 2022 (2022), p. 083C01. DOI: 10.1093/ptep/ptac097.